Phase Transformation in Poly(1-butene) upon Drawing

Koh Nakamura, Taku Aoike, Kazuto Usaka, and Tetsuo Kanamoto*

Department of Applied Chemistry, Science University of Tokyo, Kagurazaka, Shinjuku-ku, Tokyo 162-8601, Japan

Received November 6, 1998; Revised Manuscript Received March 24, 1999

ABSTRACT: Isotactic poly(1-butene) (PB-1) films, consisting either of crystal form III (solution-grown crystal mat) or I′ (melt-crystallized film under a high pressure), were drawn uniaxially by tensile draw and solid-state coextrusion in the range of room temperature to 80 °C, below their melting temperatures (T_m = 90−100 °C). The phase transformations induced by draw were characterized by WAXD and DSC. The results are discussed in terms of the effect of drawing variables on the deformation mechanism of PB-1. Tensile draw, which proceeded with a clear neck, was variable and affected by the initial crystal forms and draw temperatures. Upon the tensile draw of form I′ films, oriented unstable form II crystals were formed independently of draw temperatures. They spontaneously transformed into the stable form I, as reported. When the form III mat was tensile drawn at 80 °C, near its T_m, oriented form II crystals were obtained, whereas the draw at a lower temperature of 70 °C produced oriented form I′ crystals. Crystal form II is known to form only by crystallization from the random chain conformation, including melt, glass, and solution. Thus, the formation of the form II on tensile draw suggests that the deformation had proceeded thorough quasi-melting followed by recrystallization into the oriented form II. In contrast to the tensile draw with a neck, solid-state coextrusion, where the deformation proceeds gradually within an extrusion die, produced oriented form I′ crystals independently of the initial crystal forms and extrusion temperatures. This suggests that the deformation on solid-state coextrusion proceeded in the crystalline state. These results indicate that the draw of PB-1 proceeds either through quasi-melting/recrystallization or in the crystalline state depending on the draw technique and temperature and the crystal form of the initial starting sample.

Introduction

The physical and mechanical properties of a crystalline polymer strongly depend on the anisotropy in chain alignment and crystal forms. Thus, the plastic deformation of crystalline polymers has been extensively studied to understand the deformation mechanism and control the resultant properties of drawn products. The uniaxial drawing of bulk polymers is either inhomogeneous with a neck or homogeneous without a neck.[1,2] In the former case, the zones of micronecks are concentrated in the neck, while in the latter the zones are randomly distributed all over the sample.

Some deformation mechanisms[1−4] assume that the plastic deformation of crystalline polymers proceeds in the crystalline state. According to Peterlin,[1,2] the major deformation proceeds in three stages: plastic deformation of the lamellae due to their rotation, twining, and shear slippage, discontinuous transformation of the lamellae into a fibrous structure by micronecking, and further plastic deformation of the fibrous structure. This model explains most of the morphological changes upon drawing of crystalline polymers except the fact that the thickness of the resultant lamellae or small-angle X-ray long period (l) of drawn products is determined by the draw temperature (T_d), independently of the initial thickness of the lamellae.[5] Further, the increase of lamellae thickness with T_d can be expressed by a unique function, which is the same as that found in the effect of crystallization temperature on l.[5] This experimental finding has been difficult to explain on the basis of the deformation in the crystalline state.

An alternative deformation model assumes that the deformation can be a quasi-melting of the crystals (below the normal melting temperature) followed by oriented recrystallization, as proposed by Flory and Yoon.[6] This quasi-melting/recrystallization mechanism provides a good explanation for the observed dependence of l on T_d. In their small-angle neutron scattering studies on the tensile draw of high-density polyethylene, Sadler and Barham[7,8] concluded that, depending on the initial morphology, the lamellae deform through melting/recrystallization into an oriented fibrous structure when the draw was made above a specific temperature (70−90 °C). Further, they also showed that the deformation proceeded in the crystalline state when made below the specific temperature. Annis et al.[9] have reported that the deformation of polyethylene under pure shear proceeds by quasi-melting/recrystallization even at room temperature (RT). They believe that rising the temperature is not a requirement for partial melting to take place, and the applied stress may cause the melting of crystals followed by recrystallization during deformation.

Iso-poly(1-butene) (PB-1) exhibits four crystal modifications[10] depending on the formation conditions: forms I, twined hexagonal with a 3_1 helix;[11] I′, untwined hexagonal with a 3_1 helix;[12] II, tetragonal with an 11_3 helix;[13] and III, orthorhombic with a 4_1 helix.[12,14] When PB-1 crystallizes from the melt or glass[15] under atmospheric pressure, unstable form II crystals appear first, slowly transforming thereafter into stable form I crystals on aging at RT.[14−19] This phase transformation is accelerated by the application of stress or strain on a form II sample.[19−22] Goldbach[20,21] suggested that normal stress and molecular mobility within noncrystalline regions play a crucial role in the phase transformation. A few form II crystals were also found among the form III lamellae precipitated from a solution under a specific

* To whom correspondence should be addressed.

10.1021/ma981735f CCC: $18.00
Published on Web 06/25/1999

Table 1. Structural Characteristics for the Crystal Modifications of PB-1

form	crystal lattice	helix	unit cell dimensions (nm)			T_m (°C)	ref
			a	*b*	*c*		
I	hexagonal (twined)	3/1	1.77	1.77	0.65	120−135	11
I′	hexagonal (untwined)	3/1	1.77	1.77	0.65	90−100	12
II	tetragonal	11/3	1.46	1.46	2.12	110−120	13
III	orthorhombic	4/1	1.25	0.89	0.76	90−100	12, 14

condition.[23] These facts suggest that form II occurs only on crystallization from a random chain conformation. Thus, we assumed that the appearance of form II crystals in the as-drawn products was an indication of the occurrence of quasi-melting followed by recrystallization into form II during drawing. Further, form I′ crystals are known to form upon crystallization from the melt under a high pressure of 1500−2000 atm.[24,25] Form III and form I′ crystals have been found to form on solution crystallization[12,23] depending on the solvent, the concentration, and the crystallization temperature. Kopp et al.[14,26] have reported that the formation of PB-1 crystal modifications can be controlled by epitaxial crystallization from melt on the appropriate organic compounds.

In this paper, solution-grown crystal (SGC) mats with form III crystals[23] and high-pressure melt-crystallized (HPM) films with form I′ crystals[24,25] were drawn by solid-state coextrusion, as developed by Griswold et al.,[27] and tensile drawing. On the basis of the phase transformations upon draw characterized by wide-angle X-ray diffraction (WAXD) and differential scanning calorimetry (DSC), the effects of drawing variables on the possible deformation mechanism are discussed in an attempt to determine whether deformation proceeds in the crystalline state or through quasi-melting followed by recrystallization.

Experimental Section

Samples. The PB-1 used was Witron 0100, obtained from Shell Chemicals Ltd. It had a viscosity-average molecular weight (M_v) of 1.0×10^6 and ^{13}C NMR isotactic pentad fraction of 90%. The two samples for the draw were a solution-grown single-crystal (SGC) mat with form III crystals and a high-pressure melt-crystallized (HPM) film with form I′ crystals. SGC's were isothermally precipitated at 50 °C from a 0.2 wt % solution in isoamyl acetate. An SGC mat was obtained by slowly filtering the crystal suspension at RT followed by drying in vacuo. An HPM film was obtained by slow cooling of the PB-1 melt from 160 °C to RT under a pressure of 1600 atm.

Drawing. SGC mats and HPM films were drawn uniaxially by solid-state coextrusion[27] and conventional tensile draw in the temperature range of RT to 80 °C. For solid-state coextrusion, one or two strips were sandwiched between split billet halves of high-density or linear low-density polyethylene depending on the extrusion temperature, T_e, and the assembly was coextruded through a conical die with a nominal extrusion draw ratio (EDR) of 2 to 5. The extrusion pressure was 100−700 atm depending on EDR and extrusion temperatures. Tensile drawing was made at constant crosshead speeds, corresponding to an initial strain rate of 2/min. An EDR and tensile draw ratio (DR) were determined from the separation of ink marks preprinted on the surface of the starting sample.

Characterization. Melting behavior was measured on a Seiko-Denshi DSC-10 under an N_2 gas flow. DSC heating scans were made over a temperature range of 30−150 °C at a rate of 5 °C/min. Wide-angle X-ray diffraction (WAXD) photographs were recorded on a flat-plate camera with an imaging plate or photographic film. Diffraction profiles were also recorded by diffractometer scans in a symmetrical transmission mode on a Rigaku Gigerflex RAD-IIIA equipped with a pulse height discriminator. Ni-filtered Cu Kα radiation generated at 40 kV and 30 mA was used.

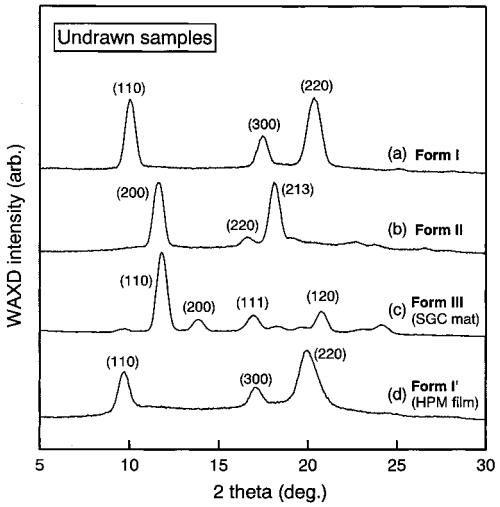

Figure 1. Typical WAXD patterns for the modifications I (a), II (b), III (c), and I′ (d) of PB-1.

Results and Discussion

Characterization of Initial Samples. The crystal forms of a sample were characterized by WAXD patterns and DSC melting behavior. Forms I and I′, having the same unit cell, cannot be distinguished by WAXD alone. However, they can be identified by electron diffraction,[12] since the former has a twined structure and the latter an untwined one. Further, the two crystal forms show different T_m's, i.e., 120−135 °C for form I and 90−100 °C for form I′. In this work, thus, these two forms were identified on the basis of the combination of WAXD patterns and DSC melting characteristics. Although forms III and I′ exhibit comparable T_m's of 90−100 °C,[12,28] these crystals can be clearly identified by their WAXD patterns. The unstable form II can be characterized by both its WAXD pattern and DSC T_m. The crystal structures and T_m's of these crystal forms are summarized in Table 1.

To determine the crystal forms of an SGC mat and an HPM film, WAXD 2θ scans and DSC heating scans were made on each sample, as shown in Figures 1 and 2, respectively. The WAXD patterns and DSC melting thermograms for form II, recorded immediately after cooling the melt from 160 °C to RT, and for form I, measured after aging form II at RT for 1 month, are also shown in these figures for comparison. The WAXD profile of an SGC mat (Figure 1c) shows a relatively strong reflection at $2\theta = 11.8°$ and weak reflections at 13.8, 16.8, and 20.7°. These can be indexed as the (110), (200), (111), and (120) reflections of form III crystals, respectively. Further, a weak reflection observed at $2\theta = 10.0°$ can be indexed as the (110) reflection of form I or form I′. Since the DSC melting thermogram of the SGC mat (Figure 2c) shows no endothermic peak corresponding to the melting of form I around 130 °C,

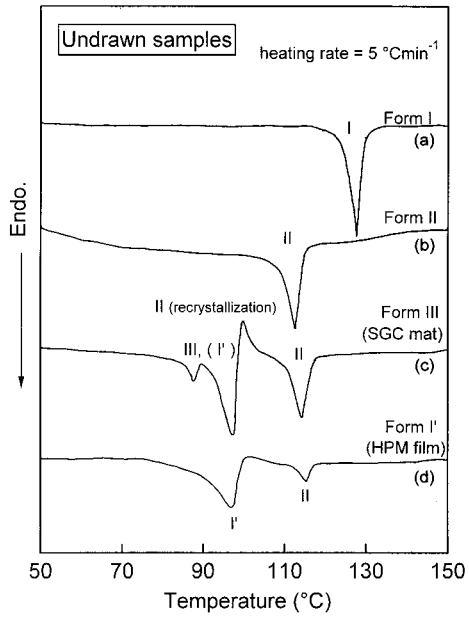

Figure 2. Typical DSC thermograms for the modifications I (a), II (b), III (c), and I′ (d) of PB-1.

this reflection is indexed as the (110) reflection of form I′. The small amount of form I′ crystals likely formed at a lower temperature while the solution was cooling to RT[23] (see Figure 1).

The DSC thermogram of an SGC mat exhibits triple endothermic peaks at 87, 98, and 115 °C and a single exothermic peak at 100 °C. Since the T_m of form III crystals is 90−100 °C (see Table 1), the major endothermic peak at 98 °C is ascribed to the melting of form III crystals, which are predominant in the SGC mat, as determined by the WAXD. The sharp exothermic peak at 100 °C, following the melting of major form III crystals and a small amount of form I′ ones, is due to recrystallization into form II crystals.[29] The endothermic peak around 115 °C is due to the melting of the recrystallized form II crystals. The origin of the small endothermic peak at the lower temperature of 87 °C is not clear. Nevertheless, this low T_m may be ascribed to the melting of disordered crystals formed from the less stereoregular component or that of thin crystals formed at a lower temperature while the solution was cooling.

The WAXD profile of an HPM film (Figure 1d) shows major peaks at $2\theta = 10.0$, 17.0, and 19.9°, which are respectively indexed as the (110), (300), and (220) reflections of form I or I′. The fact that the DSC thermogram of the HPM film (Figure 2d) does not exhibit the melting peak around 130 °C that is characteristic for the form I indicates that this sample consists of form I′ crystals. Thus, the endothermic peaks at 97 and 118 °C are ascribed to the melting of forms I′ and II, respectively. The broad exotherm around 100 °C is ascribed to the recrystallization of the melt into form II crystals during the DSC heating scan. This is supported by the fact that the exothermic peak became clearer on DSC heating at a lower rate. As discussed, WAXD and DSC results revealed that the SGC mat consists predominantly of form III crystals with a small amount of form I′ ones, and the HPM film is composed of form I′ crystals.

WAXD photographs of an SGC mat and an HPM film are shown in Figure 3. The incident beam was directed perpendicularly to the wide surfaces (through view) of the samples. The WAXD photograph of the SGC mat, obtained with the incident beam parallel to the wide surface (edge view, not shown), shows the (hk0) reflections of form III crystals on the meridian. Further, a small-angle X-ray long-period scattering appeared on the equator. These facts show that the single-crystal lamellae are stacked parallel to the wide surface of the mat, and the molecular chains are preferentially oriented perpendicularly to the mat surface. In contrast, both through and edge views of the WAXD for the HPM film exhibited uniform Debye−Scherrer rings showing form I′ crystals are randomly oriented within the film.

Drawing. PB-1 generally shows only low ductility in the solid state. Ball and Porter[30] and Aharoni and Sibilia[31] reported that no continuous extrudates could be obtained on solid-state extrusion of PB-1 with a variety of initial morphologies. However, Tasaka et al.[32] succeeded in the preparation of continuous extrudates with EDR ≤ 5 by applying a special extrusion technique. A film partially preoriented (×1.5) by calendering was buried within a lead billet, and the assembly was coextruded through a die, simultaneously applying a pulling force on the coextrudate. Tensile drawing is likely easier than solid-state extrusion for the drawing of PB-1. For the tensile drawing of an aged sample, Oda et al.[18] reported DR ≤ 4. Yang and Geil[22] report that a melt-crystallized, fresh PB-1 sample with the form II exhibits a higher ductility than that of an aged sample with form I and that the former could be drawn to DR ≤ 8.5. In this work, both the SGC mat and the HPM film could easily be drawn to a draw ratio of 3−5 by both solid-state coextrusion and tensile drawing. Thus, the two starting samples were drawn to a constant draw ratio of 3−3.5 in the temperature range of RT to 80 °C.

Solid-State Coextrusion. WAXD photographs of extrudates with an EDR of 3−3.5, prepared from the two initial morphologies at 80 °C, about 10−20 °C below their DSC melting peak temperatures, are shown in Figure 3. The fiber patterns were recorded both immediately after extrusion (Figure 3b,e) and after 1 day kept at RT (Figure 3c,f). The X-ray exposure time was 5−30 min depending on the recording systems of an imaging plate or photographic film. The aging of the extrudates at RT for 1 day caused no changes in the diffraction patterns, indicating that the new oriented crystals formed upon solid-state coextrusion were stable at RT. These extrudates with an EDR of ∼3 exhibit a fairly high chain orientation.

The WAXD photograph of an extrudate from an SGC mat, prepared at $T_e = 80$ °C (Figure 3b), shows a weak (110) reflection arc from the initial form III crystals with the intensity maximum on the meridian. This suggests that a small fraction of the form III crystals, initially oriented perpendicularly to the draw axis, survived even after extrusion, probably due to interlamellae slippage along the draw direction which is parallel to the wide surfaces of lamellae. Indeed, solution-grown single crystals generally have only a few tie molecules connecting the lamellae, and such slippage of parallel lamellae along their surfaces might therefore occur rather easily. Despite the existence of a weak (110) reflection from the initial form III crystals, all the strong reflections are indexed as (hkl) reflections of form I or I′, as shown in the photograph. Further, no reflection of form II was observed for the extrudates from an SGC mat, suggesting that the deformation proceeded in the crystalline state. As the two crystal forms cannot be

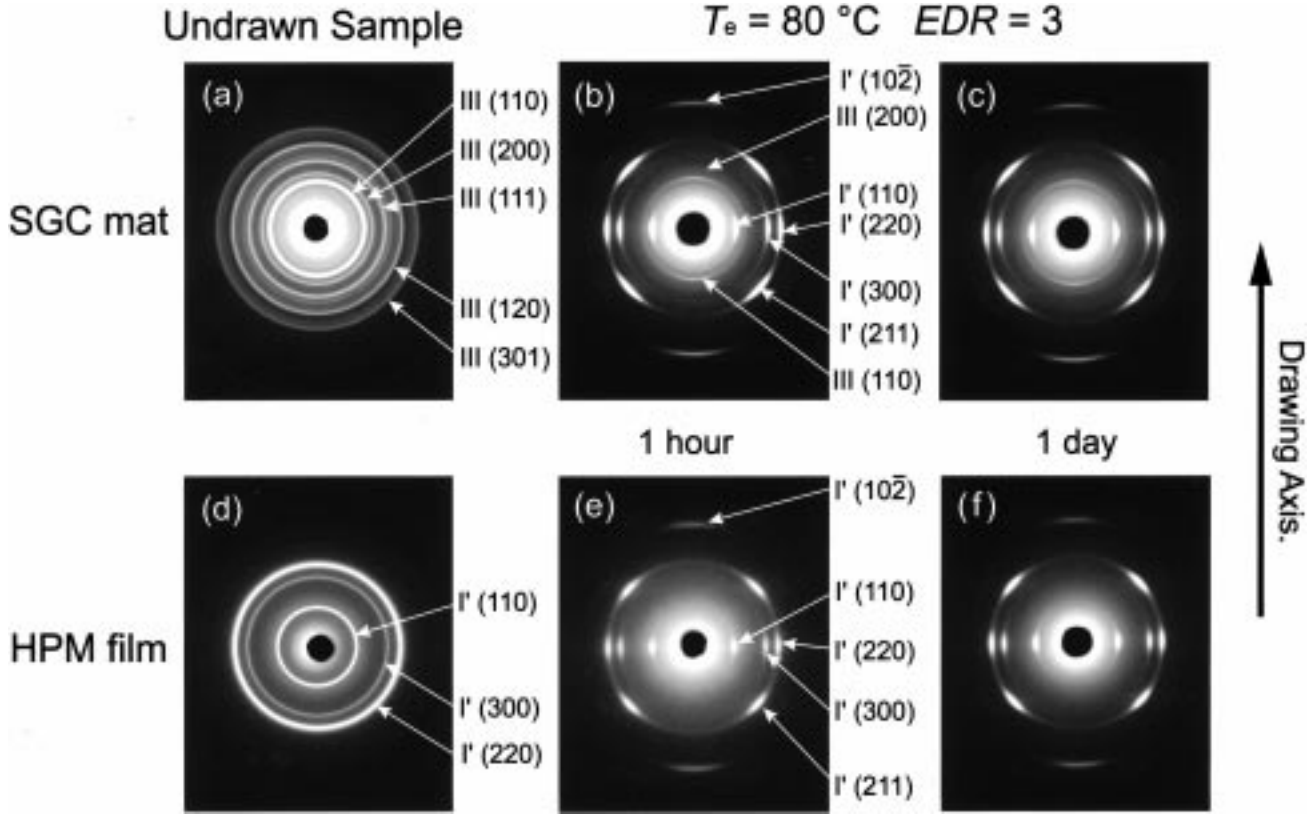

Figure 3. WAXD photographs of an initial SGC mat and an HPM film and their extrudates with an EDR = 3, prepared at 80 °C. The incident X-ray beam was perpendicular to the wide surfaces of samples. (a) An SGC mat; (b) an extrudate of the SGC mat recorded soon after extrusion; (c) the sample (b) recorded after aging at RT for 1 day; (d) an HPM film; (e) an extrudate of the HPM film recorded immediately after extrusion; and (f) the sample (e) recorded after aging at RT for 1 day.

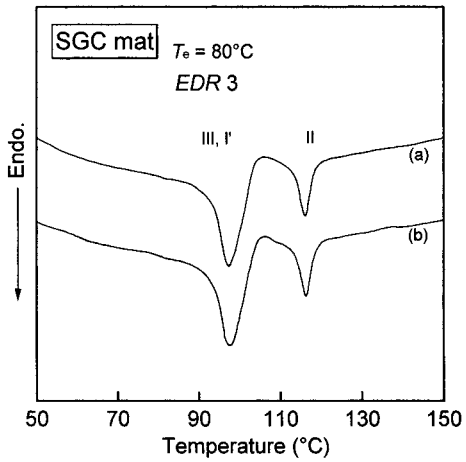

Figure 4. DSC thermograms for a coextruded SGC mat with an EDR 3, prepared at 80 °C. Measured immediately after extrusion (a) and after aging at RT for 1 day (b).

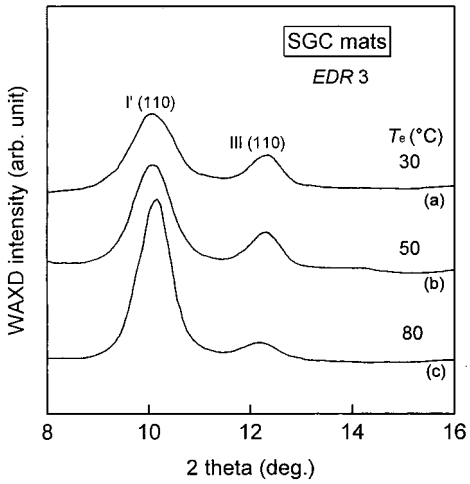

Figure 5. WAXD equatorial scans for the extrudates from SGC mats with an EDR of 3, prepared at T_e of 30 (a), 50 (b), and 80 °C (c). The patterns were obtained immediately after extrusion with the incident beam perpendicular to the wide surfaces of samples.

distinguished by WAXD alone, the melting behavior of the extrudate was examined.

Figure 4 shows DSC thermograms of the extrudate prepared at T_e = 80 °C from an SGC mat, recorded immediately after coextrusion (Figure 4a) and after keeping at RT for 1 day (Figure 4b). No aging effect was observed. Neither of them shows a melting peak around 130 °C, revealing the absence of form I crystals. This indicates that the major crystal modification is the form I′ for the coextrudate. Thus, the endothermic peaks at 97 and 114 °C in Figure 4 are respectively ascribed to the melting of form I′ crystals plus a small amount of the initial form III crystals and the melting of the recrystallized form II crystals during heating. These observations reveal that most of the initially form III crystals of the SGC mat transformed into the form I′ on extrusion at 80 °C.

The effect of T_e on the phase transformation upon coextrusion of an SGC mat (form III) was examined by equatorial X-ray diffractometer scans on the coextrudates prepared at T_e = 30, 50, and 80 °C, as shown in Figure 5. Although the (110) reflection of the new form I′ crystals became broader and weaker with decreasing T_e, the majority of the initial form III crystals trans-

formed into form I′ independently of T_e. Such a phase change is consistent with the prediction of Saraf and Porter[33] that the phase transformation induced by solid-state deformation proceeds to the direction of decreasing the cross-sectional area of a chain within the unit cell.

The WAXD pattern of the extrudate prepared at T_e = 80 °C from a HPM film (Figure 3e) is basically the same as that of the extrudate from a SGC mat, except that the former shows a slightly higher chain orientation than the latter (Figure 3b). The higher chain orientation of the former suggests that the draw stress was more homogeneously transmitted within the HPM film than the SGC mat, since a melt-crystallized film generally has a highly entangled network, as opposed to an SGC mat, in which each lamella was basically isolated.

The combined results of WAXD and DSC analyses showed that this HPM extrudate prepared at T_e = 80 °C consisted of oriented form I′ crystals as well. Further, the coextrusion of an HPM film at a lower T_e of RT to 70 °C also produced an oriented form I′. It is noted that no form II crystals formed on solid-state coextrusion at a $T_e \leq 80$ °C for the HPM film or for the SGC mat. This suggests that both form I′ and form III crystals reorganize into oriented form I′ crystals upon coextrusion in the crystalline state.

Tensile Drawing. Significant differences in draw behavior have been observed between tensile draw and solid-state coextrusion of the SGC mat and HPM film. It should be remembered that solid-state extrusion proceeds in homogeneous deformation within an extrusion die, whereas the tensile draw of these samples proceeded by the formation of a clear neck followed by propagation on drawing in the temperature range of RT to 80 °C. The draw ratio after the neck had propagated in the whole sample portion was 3−4 depending on draw temperatures and initial morphologies. Further draw led to sample failure. Therefore, each sample was tensile drawn to a DR of 3−3.5, and the phase change induced by the deformation was characterized.

SGC mats were tensile drawn at T_d = 70 and 80 °C, 10−30 °C below the DSC T_m. No tensile draw was achieved below $T_d \leq 60$ °C for this sample. WAXD diffractometer scans on the equator and DSC thermograms for the drawn products are shown in Figures 6 and 7, respectively. They were measured immediately after draw and after aging at RT for 1 day. The WAXD profile of the sample drawn at a T_d = 70 °C shows reflections at 2θ = 10.0, 12.4, and 14.2°. They can be indexed as the (110) reflection of the form I or I′ and the (110) and (200) reflections of the initial form III, respectively, as shown in Figure 6. Neither the DSC melting curve recorded immediately after draw (Figure 7a) nor that examined after aging at RT (Figure 7b) showed the melting endotherm around 130 °C, which is characteristic of the melting of form I crystals. This indicates the absence of form I crystals in the SGC mat tensile drawn at 70 °C even after aging at RT. Thus, the reflection at 2θ = 10.0° in Figure 6a,b is ascribed to the (110) reflection of form I′ crystals. These results suggest that, upon tensile drawing of an SGC mat at 70 °C, part of the initially form III crystals transformed into form I′ crystals in the crystalline state.

The tensile draw of an SGC mat at a higher T_d of 80 °C, near the T_m (see Table 1), is markedly different from the draw at a low T_d of 70 °C. The equatorial WAXD profile of the SGC mat drawn at T_d = 80 °C (Figure 6c),

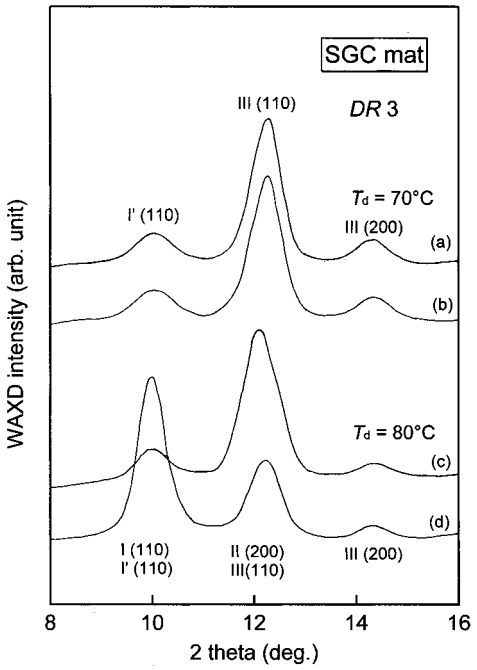

Figure 6. WAXD equatorial scans for (a) an SGC mat tensile drawn at 70 °C to a DR of 3, recorded soon after drawing; (b) the sample (a) recorded after aging at RT for 1 day; (c) an SGC mat tensile drawn at 80 °C to a DR of 3, recorded soon after drawing; and (d) the sample (c) recorded 1 day after drawing. Note a significant aging effect for the sample drawn at T_d = 80 °C.

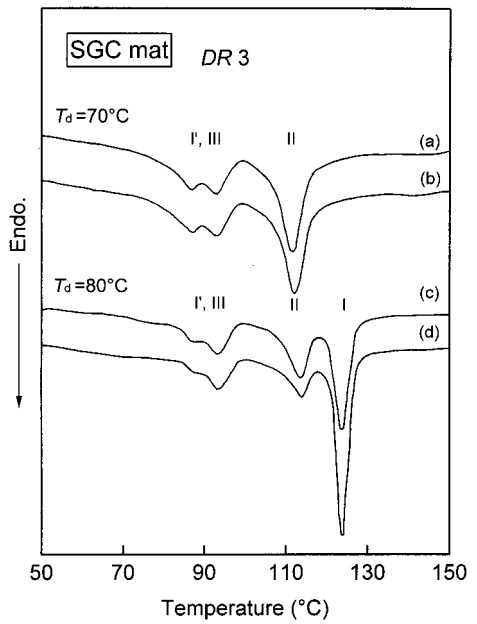

Figure 7. DSC thermograms for the SGC mats tensile drawn to a DR 3 at 70 °C (a, b) and at 80 °C (c, d). Measurements were made immediately after draw (a, c) and after aging at RT for 1 day (b, d). Note a significant effect of aging on the thermogram for the sample drawn at T_d = 80 °C.

recorded immediately after draw, shows reflections at 2θ = 10.0, 12.2, and 14.4°. They can be indexed as the (110) reflection of form I or I′, (200) of form II and/or (110) of form III, and (200) of form III, respectively. As is known, only the form II modification is unstable and spontaneously transforms into the form I. Thus, further assignments of these crystal forms were made on the basis of significant effects of aging at RT on the WAXD pattern and DSC melting behavior. Upon standing the

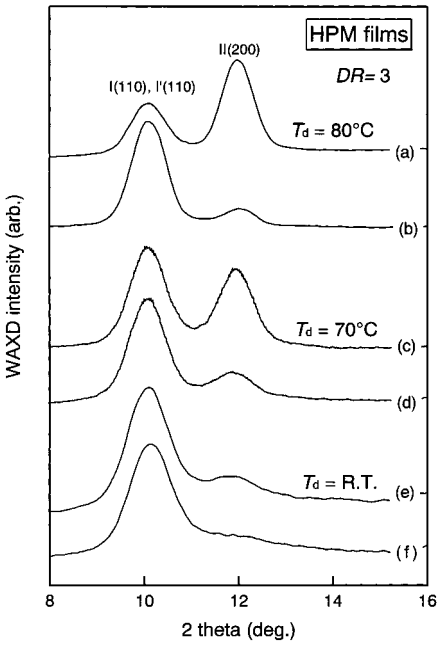

Figure 8. WAXD equatorial scans for the HPM films tensile drawn at 80 °C (a, b), at 70 °C (c, d), and at RT (e, f). (a), (c), and (e) were recorded immediately after draw and (b), (d), and (f) after aging at RT for 1 day.

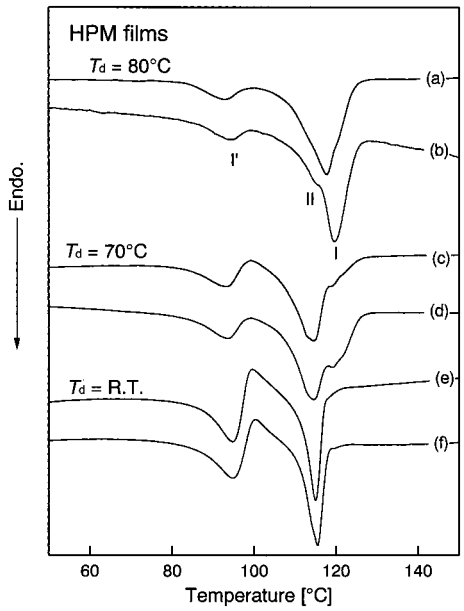

Figure 9. DSC thermograms for the HPM films tensile-drawn to a DR of 3 at 80 °C(a, b), at 70 °C (c, d), and at RT (e, f). (a), (c), and (e) were recorded immediately after draw and (b), (d), and (f) after aging at RT for 1 day.

drawn product at RT for 1 day, the intensity of the reflection at $2\theta = 10.0°$ markedly increased at the expense of the peak intensity at $2\theta = 12.2°$. This suggests that form II crystals existed in the as-drawn, fresh product transformed into form I crystals on aging at RT. Consistent with this, a comparison of DSC thermograms of the fresh and aged samples in Figure 7 shows that the melting peak at 125 °C for form I crystals had grown upon aging at RT at the expense of the 113 °C peak for the melting of form II crystals. Further, the fact that the DSC thermogram of the as-drawn SGC mat (Figure 7c) already exhibits a melting peak for form I crystals at 125 °C indicates that the form II crystals formed upon draw rapidly transformed into form I crystals during draw or in a short time before the DSC measurement was made. Indeed, Oda et al.[18] and Yang and Geil[22] found that such a phase transformation is accelerated by the chain orientation.

These WAXD and DSC results reveal that the tensile draws of SGC mats at $T_d = 80$ and 70 °C are significantly different from each other. More specifically, the results have an important implication concerning the deformation mechanisms. The tensile draw of an SGC mat at $T_d = 70$ °C proceeded in the crystalline state, whereas that at $T_d = 80$ °C proceeded by quasi-melting of the initial form III followed by recrystallization into form II. The latter mechanism is likely connected to the heat evolved on neck deformation[34] and partly to the depression of the melting temperature of a crystalline polymer by the application of a tensile load, as extensively discussed by Smith.[35] A similar effect of T_d on the deformation mechanism has been reported by Sadler and Barham[7,8] in their study on tensile drawing of high-density polyethylene by small-angle neutron scattering.

The effect of T_d on tensile draw was examined also for an HPM film (form I′). Figure 8 shows WAXD equatorial profiles of HPM films drawn at $T_d = 80$ °C, 70 °C, and RT. These profiles were recorded immediately after draw and also after aging at RT for 1 day. All the as-drawn products show reflections at $2\theta = 10.0$ and 12.2°. The intensity of the reflection at 10.0° increased upon aging at the expense of intensity of the reflection at 12.2°, confirming that these reflections correspond to the (110) of form I and/or form I′ crystals and the (200) of form II crystals, respectively. The fresh sample prepared at $T_d = 80$ °C shows a strong (200) reflection of form II crystals and a weaker (110) reflection of form I and/or form I′ crystals, suggesting that a major fraction of the initial form I′ crystals transformed into form II upon drawing through quasi-melting followed by recrystallization. The relative intensity of the (200) reflection of form II for a fresh sample became weaker with decreasing T_d, which indicates that the amount of form II crystals formed upon draw decreased with decreasing T_d. It should be noted, however, that a fresh sample prepared at 70 °C shows a strong (200) reflection from form II crystals, which were not formed upon the tensile drawing of an SGC mat (form III) at the same temperature (see Figures 6 and 7). Further, the appearance of a weak (200) reflection of form II for the sample drawn at RT suggests that at least a small fraction of the initial form I′ crystals was deformed through quasi-melting followed by recrystallization even at a low T_d, about 60−70 °C below the static T_m of the form I′. The significance of these results is that the deformation mode for the tensile drawing of PB-1 depends not only on the T_d but also on the initial crystal form of a sample.

As the WAXD patterns gave no information on the relative amounts of form I and form I′ crystals existing in these samples, their DSC melting curves were obtained as shown in Figure 9. The thermogram of a fresh sample drawn at $T_d = 80$ °C shows three endotherms, i.e., a small peak at 95 °C, a fairly large peak at 115 °C, and a shoulder around 120 °C, corresponding to the melting of form I′, form II, and form I crystals, respectively. Upon aging at RT for 1 day, the 120 °C peak grew at the expense of the 115 °C peak and became a major peak (Figure 9b) due to the transformation of form II crystals into form I crystals. The T_m of this form

I was about 5 °C lower that that of the form I formed on drawing of an SGC mat at the same T_d of 80 °C (Figure 7d). A similar change in the form II T_m has been reported.[22] These DSC results confirm the WAXD results which suggested that, upon tensile drawing of an HPM film at T_d = 80 °C, a substantial fraction of the initial form I′ crystals transformed into form II crystals, yet only a small amount of form I′ crystals still existed within the drawn product.

When an HPM film was drawn at a lower T_d, the relative areas of both melting peaks at 95 and 115 °C increased, whereas that at 120 °C decreased. The DSC curve of the sample drawn at RT showed no significant change upon aging at RT for 1 day. It showed two melting peaks at 95 and 115 °C due to the melting of form I′ and form II crystals, respectively. A closer inspection of the thermograms, however, revealed the existence of a small endothermic tail at the higher temperature side of the 115 °C peak due to the melting of a small amount of form I crystals. These DSC results are consistent with the WAXD patterns in Figure 8.

The results discussed above indicate that solid-state coextrusion of both an SGC mat (form III) and an HPM film (form I′) gave oriented samples with form I′ crystals independently of T_e at RT to 80 °C, suggesting that homogeneous deformation under the shear and extensional flow fields[36] proceeds in the crystalline state. In contrast, the tensile draw with a neck was more variable and depended on the T_d and initial sample morphology. The tensile draw of both an SGC mat and an HPM film at a higher T_d of 80 °C produced an oriented sample with form II crystals, indicating that the draw proceeded through quasi-melting followed by recrystallization into the unstable form II. However, the tensile draw of an SGC mat at a lower T_d of 70 °C produced an oriented form I′, which seems to indicate that the deformation proceeded in the crystalline state. The effect of T_d on the deformation mode was significantly different between an SGC mat and an HPM film. The latter produced form II crystals upon draw even in the lower T_d range of RT to 70 °C, although the amount of form II crystals generated upon draw decreased and that of the oriented form I′ crystals increased when drawn at a lower T_d.

The tensile draw of an SGC mat (form III) and an HPM film (form I′) proceeded with a clear neck independently of T_d, which might evolve a significant heat of deformation depending on the draw rate. Thus, it was expected that the marked difference in the tensile draw behavior of the two morphologies might be connected with the temperature rise at the neck portion. Figure 10 shows nominal stress vs strain curves for the tensile draw of an HPM film and an SGC mat at 70 °C. It should be remembered that, despite a comparable T_m (90−100 °C) for the two samples, form II crystals were generated only for the HPM film with form I′ crystals upon tensile draw at this T_d. The two morphologies exhibited no significant differences in the stress/strain curves, suggesting that the heat evolved at the neck might be comparable. This suggests that the difference in deformation mode for the tensile draw of the two initial morphologies, having a comparable T_m, is likely related to the nature of the two crystal forms (form III vs form I′) and may not be directly related to the actual temperatures at the neck regions. The routes for the phase transformations in PB-1, depending on crystallization and deformation conditions, are summarized in Figure 11. The bold arrows indicate the transformation routes observed in this work, as discussed above.

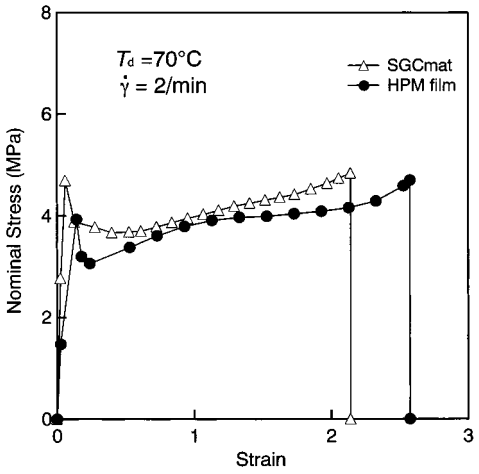

Figure 10. Nominal stress/strain curves for tensile drawing of an SGC mat (form III) and an HPM film (form I′) recorded at 70 °C.

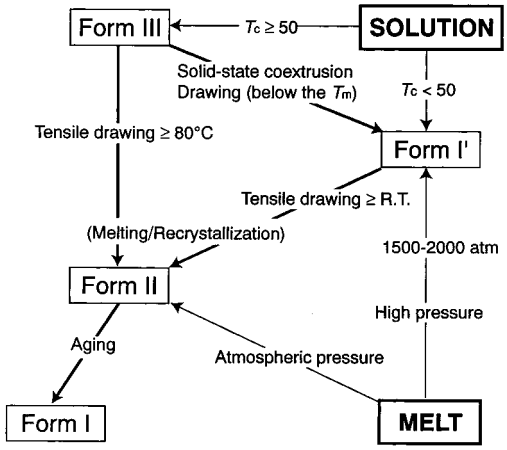

Figure 11. Schematics showing routes for the formation and transformations of crystal modifications on crystallization and drawing of PB-1.

Conclusions

The phase transformations upon the drawing of PB-1 samples with either form I′ (HPM film) or form III crystals (SGC mat) were characterized by WAXD and DSC, as summarized in Figure 11. The draw was made by solid-state coextrusion and tensile draw at RT to 80 °C. Drawing variables had a significant effect on the deformation mechanism. Solid-state coextrusion of these samples produced oriented tapes with form I′ independently of the initial crystal forms and coextrusion temperatures, T_e. This probably means that the deformation proceeded in the crystalline state. The results for tensile draw with a neck for these samples were more variable. The tensile draw of the form III SGC mat at a higher T_d of 80 °C, near the T_m of 90−100 °C, produced an oriented tape with unstable form II crystals, which spontaneously transformed into the stable form I. However, the drawing of the mat at a lower T_d of 70 °C yielded an oriented tape with form I′ crystals. In contrast to the SGC mat, the tensile draw of the form I′ HPM film was found to produce oriented tapes with form II crystals independently of T_d, although the amount of form II crystals generated decreased with decreasing the T_d. The formation of form II crystals

suggests that the deformation at the neck likely proceeded through quasi-melting of the initial crystals followed by recrystallization into the form II. Since the formation of form II crystals was observed only for the tensile draw with a sharp neck, the temperature rise at the neck portion and the applied tensile load are likely to be important factors leading to such a deformation mode. These results show that the deformation of PB-1 depends on the crystal forms of an initial sample as well as the draw temperature and technique.

References and Notes

(1) Peterlin, A. *J. Polym. Sci.* **1996**, *C15*, 427.
(2) Peterlin, A. *J. Mater. Sci.* **1971**, *6*, 490.
(3) Crist, B. *Polym. Commun.* **1989**, *30*, 69.
(4) Hay, I. L.; Keller, A. *Kolloid Z. Z. Polym.* **1965**, *204*, 43.
(5) Meinel, G.; Morosoff, N.; Peterlin, A. *J. Polym. Sci.* **1970**, *A-2*, 8, 1723.
(6) Flory, P. J.; Yoon, D. Y. *Nature* **1978**, *272*, 226.
(7) Sadler D. M.; Barham, P. J. *Polymer* **1990**, *31*, 36.
(8) Sadler D. M.; Barham, P. J. *Polymer* **1990**, *31*, 43.
(9) Annis, B. K.; Strizak, J.; Wignall, G. D.; Alamo, R. G.; Mandelkern, L. *Polymer* **1996**, *37*, 137.
(10) Luciani, L.; Sepälä, J.; Löfgren, B. *Prog. Polym. Sci.* **1988**, *13*, 37.
(11) Natta, G.; Corradini, P.; Bassi, I. W. *Nuovo Cimento Suppl.* **1960**, *15*, 52.
(12) Miller, R. L.; Holland, V. F. *Polym. Lett.* **1964**, *2*, 519.
(13) Turner-Jones, A. *J. Polym. Sci.* **1963**, *B18*, 455.
(14) Kopp, S.; Wittmann, J. C.; Lotz, B. *Polymer* **1994**, *35*, 908.
(15) Hsu, C. C.; Geil, P. H. *J. Macromol. Sci. Phys.* **1986**, *B25*, 433.
(16) Dannuso, F.; Gianotti, G. *Macromol. Chem.* **1963**, *61*, 139.
(17) Boor Jr., J.; Mitchell, J. C. *J. Polym. Sci.* **1963**, *A1*, 59.
(18) Oda, T.; Maeda, M.; Hibi, S.; Watanabe, S. *Kobunshi Ronbunshu* **1974**, *31*, 129.
(19) Asada, T.; Sasada, J.; Onogi, S. *Polym. J.* **1972**, *3*, 350.
(20) Goldbach, G. *Angew. Makromol. Chem.* **1973**, *29/30*, 213.
(21) Goldbach, G. *Angew. Makromol. Chem.* **1974**, *39*, 175.
(22) Yang, Y.; Geil, P. H. *Macromol. Chem.* **1985**, *186*, 1961.
(23) Holland, V. F.; Miller, R. L. *J. Appl. Phys.* **1964**, *35*, 3241.
(24) Armeniades, C. D.; Bear, E. *J. Macromol. Sci., Phys.* **1967**, *B-1*, 2, 309.
(25) Nakafuku, C.; Miyaki, T. *Polymer* **1983**, *24*, 141.
(26) Kopp, S.; Wittmann, J. C.; Lotz, B. *Polymer* **1994**, *35*, 917.
(27) Griswold, P. D.; Zachariades, A. E.; Porter, R. S. *Polym. Eng. Sci.* **1982**, *18*, 861.
(28) Clampitt, B. H.; Hughes, R. H. *J. Polym. Sci.* **1964**, *C6*, 43.
(29) Geacintov, C.; Schotland, R. S.; Miles, R. B. *J. Polym. Sci.* **1964**, *C6*, 197.
(30) Ball, R.; Porter, R. S. *Polym. Lett.* **1977**, *15*, 519.
(31) Aharoni, S. M.; Sibilia, J. P. *J. Appl. Polym. Sci.* **1979**, *23*, 133.
(32) Tasaka, S.; Suzuki, T.; Miyata, S. *Kobunshi Ronbunshu* **1982**, *39*, 127.
(33) Saraf, R. F.; Porter, R. S. *J. Polym. Sci.* **1988**, *B26*, 1049.
(34) Vincent, P. *Polymer* **1960**, *1*, 7.
(35) Smith Jr., K. *J. Comput. Theor. Polym. Sci.* **1997**, *7*, 139.
(36) Kanamoto, T.; Zachariades, A. E.; Porter, R. S. *Polym. J.* **1979**, *11*, 307.

MA981735F